MITSUBISHI ELECTRIC RESEARCH LABORATORIES
https://www.merl.com

Hole transport mechanism at high temperatures in p-GaN/AlGaN/GaN Heterostructure

Sikder, Bejoy; Hossain, Toiyob; Xie, Qingyun; Niroula, john; Rajput, Nitul S.; Teo, Koon Hoo; Amano, Hiroshi; Palacios, Tomas; Chowdhury, Nadim

TR2025-014 January 28, 2025

Abstract

This letter reports an investigation of hole transport in p-GaN/AlGaN/GaN heterostructures through experimental and theoretical analyses under varied conditions. Highly non-linear current-voltage (I-V) characteristics, obtained via the linear transmission line method (LTLM) measurements, are utilized for this study. At low bias voltage, the transport can be ascribed to the Schottky nature of the contact, while at high bias, the conduction is observed to be governed by space-charge limited current (SCLC). The Schottky characteristics (Schottky Barrier height and non-ideality factor) and the SCLC exponent were analyzed for devices with varying contact spacings and at different high temperatures. The SCLC exponent, m ranges from 2 Less Than or Equal m Less Than or Equal 4 depending on the applied voltage range, revealing the existence of the trap states in the channel region. The findings of this work indicate that the charge injection, field-induced ionization, and trap states in the p-GaN channel are critical factors in the current transport of p-GaN/AlGaN/GaN heterostructure.

Applied Physics Letters 2025

© 2025 MERL. This work may not be copied or reproduced in whole or in part for any commercial purpose. Permission to copy in whole or in part without payment of fee is granted for nonprofit educational and research purposes provided that all such whole or partial copies include the following: a notice that such copying is by permission of Mitsubishi Electric Research Laboratories, Inc.; an acknowledgment of the authors and individual contributions to the work; and all applicable portions of the copyright notice. Copying, reproduction, or republishing for any other purpose shall require a license with payment of fee to Mitsubishi Electric Research Laboratories, Inc. All rights reserved.

Mitsubishi Electric Research Laboratories, Inc.
201 Broadway, Cambridge, Massachusetts 02139

Hole Transport Mechanism at high temperatures in p-GaN/AlGaN/GaN Heterostructure

Bejoy Sikder,[1, a)] Toiyob Hossain,[1, a)] Qingyun Xie,[2] John Niroula,[2] Nitul S. Rajput,[3] Koon Hoo Teo,[4] Hiroshi Amano,[5] Tomás Palacios,[2] and Nadim Chowdhury*[1]
[1)] *Department of Electrical and Electronic Engineering, Bangladesh University of Engineering and Technology, Dhaka-1205, Bangladesh*
[2)] *Microsystems Technology Laboratories, Massachusetts Institute of Technology, Cambridge MA 02139 U.S.A.*
[3)] *Advanced Materials Research Center, Technology Innovation Institute, Abu Dhabi P.O. Box 9639 U.A.E.*
[4)] *Mitsubishi Electric Research Labs, Cambridge, MA 02139, U.S.A.*
[5)] *Nagoya University, Furo-cho, Chikusa-ku, Nagoya, 464-8601, Japan.*

(*Author to whom correspondence should be addressed: nadim@eee.buet.ac.bd)

(Dated: 1 June 2024)

This letter reports an investigation of hole transport in p-GaN/AlGaN/GaN heterostructures through experimental and theoretical analyses under varied conditions. Highly non-linear current-voltage (I-V) characteristics, obtained via the linear transmission line method (LTLM) measurements, are utilized for this study. At low bias voltage, the transport can be ascribed to the Schottky nature of the contact, while at high bias, the conduction is observed to be governed by space-charge limited current (SCLC). The Schottky characteristics (Schottky Barrier height and non-ideality factor) and the SCLC exponent were analyzed for devices with varying contact spacings and at different high temperatures. The SCLC exponent, m ranges from $2 \leq m \leq 4$ depending on the applied voltage range, revealing the existence of the trap states in the channel region. The findings of this work indicate that the charge injection, field-induced ionization, and trap states in the p-GaN channel are critical factors in the current transport of p-GaN/AlGaN/GaN heterostructure.

In recent years, there has been a growing interest in GaN-based integrated circuits owing to their essential usage in driver circuitry for power electronics.[1–3] The existing multichip approach, which involves a Si control circuit combined with a GaN power circuit, has encountered limitations in terms of operating frequency, inability to operate in harsh environments and circuit complexity.[4] Another popular approach to GaN driver circuits is the use of the directly coupled field effect transistors with E/D mode GaN HEMT.[5,6] However, they suffer from significant static power dissipation. Consequently, an all-GaN-CMOS technology would significantly advance power and mixed-signal integrated circuits and high-speed power converters. Therefore, it is imperative to develop a p-GaN device that can be monolithically integrated with the existing established n-FETs. In pursuit of this objective, a number of p-GaN devices have been proposed over the years.[7–11] These p-GaN FETs typically use p-GaN/AlGaN/UID (Unintentionally Doped) GaN heterostructures as their elemental unit. Additionally, p-GaN gate HEMT is a commercially available technology for power switching applications that employ p-type GaN layer in the gate stack.

Nevertheless, the primary constraints associated with devices based on p-GaN stem from factors such as the limited activation of Mg-acceptors ($\sim 1-2\%$) at room temperature due to a high ionization energy ($\sim$ 170 meV), as well as low hole mobility (10-20 $\mathrm{cm^2/V\cdot s}$).[12,13] Due to incomplete ionization, most of the Mg-acceptors behave like deep-level states resulting in interesting carrier transport mechanisms such as deep-level defect mediated conduction. 2D-variable range hopping also occurs in such devices depending on the type of metal/p-GaN interface.[14–16] Space-charge effect is another plausible transport mechanism in systems with low-doping capability that leads to nonlinear, non-exponential I-V characteristics with the relationship: $I \propto V_A^m$.[17–20] Despite extensive research efforts primarily directed towards the improvement of p-GaN device performance, there remains a notable absence of in-depth and exhaustive investigations into the characteristics of hole transport and the underlying mechanisms governing hole current conduction within these systems. Moreover, such a study is also important to understand the reliability issues and high temperature performances of p-GaN gate HEMT as reported in[21–24]. Recently, few works have been reported shedding light on the origin of the Two-Dimensional Hole gas (2DHG) and its electrical and transport characteristics, such as carrier distribution and mobility.[25,26] These studies have primarily focused on material parameters pertaining to the transport properties. However, a comprehensive device-based study of the current conduction mechanism in a p-GaN/AlGaN/UID GaN heterostructure under different bias conditions and temperatures is required for the design and performance optimization of p-GaN-based device.

In this letter, an experimental and theoretical analysis of the hole transport mechanism in p-GaN/AlGaN/UID GaN heterostructures under varying bias and temperature conditions has been reported. Current is measured in the horizontal direction, i.e., contact-to-contact conduction. In general, two distinct transport mechanisms are observed at separate bias regions. Thermionic emission is observed in low voltage bias (V_A < 1 V), while space charge limited current conduction (SCLC) hypothesis is confirmed at higher applied bias (V_A > 1 V).

It should be mentioned that hole transport in a p-GaN/AlGaN/GaN heterostructure comprises two components- transport within the p-GaN layer and transport

---

[a)] These authors contributed equally

of the 2DHG at the p-GaN/AlGaN interface. Nonetheless, since the data analyzed in this study aggregates the current from the totality of the two components, this analysis indicates that the bias-dependent coexistence of thermionic emission and SCLC characterizes the overall hole transport in the p-GaN/AlGaN/GaN heterostructure. Such studies are important and meaningful for understanding the existing performance limitations of p-GaN/AlGaN/GaN heterostructures.

A standard p-GaN/AlGaN/GaN epitaxy has been used for this study. Fig.1(a) presents the schematic of the heterostructure. Similar epitaxial structures have been reported previously in several p-channel GaN transistors to realize GaN CMOS technology.[27–29] Fig.1(b) shows the simulated energy band diagram of the epitaxial layer. This study employs a Ru contact integrated p-channel device, chosen for its compatibility with the Si-CMOS process, making it well-suited for use in CMOS foundries.[29–31] The LTLM technique proposed by Shockley has been used to characterize the contact resistance of the p-GaN/AlGaN/GaN heterostructure with Ru contact. Additionally, the Ru/p-GaN interface (after annealing at 500°C) was characterized using transmission electron microscopy (TEM)(Fig.1(c)). In Fig.1(d), the Linear TLM (LTLM) test structure used in this work is illustrated. d represents the contact spacing for LTLM. A Scanning Electron Microscope (SEM) image of the top view of the LTLM test structure is depicted in Fig.1(f). The details of the epitaxial growth and contact formation of the structure, along with necessary equations for contact and sheet resistance extractions, are given in.[32] Fig. 1(e) illustrates the various elements contributing to the overall resistance of the LTLM structure. The total resistance (R_T) is given by: $R_T = 2R_m + 2R_c + R_{channel} \approx 2R_c + R_{channel} = 2R_c + R_{sh} \times (d/W)$. Here R_m, R_c, $R_{channel}$ and R_{sh} are the resistances of the metallic conductor, contact resistance, channel, and sheet resistance, respectively, d is the contact spacing and W is the width of LTLM structure. R_m has been considered negligible compared to R_c and $R_{channel}$. R_c and R_{sh} have been obtained by fitting relevant equations to the R_T *vs.* d relationships.[32] The measured $I-V$ data *vs.* temperature are depicted in Fig.1(g), where the $I-V$ characteristics of such devices are non-ohmic (non-linear). The non-linearity of $I-V$ is also evident from the extracted R_c and $R_{channel}$, both of which are strong functions of applied bias[Fig.1(h)]. At a low bias, the contact resistance is higher; at a higher bias, the channel resistance starts to dominate. The voltage at which the channel starts to dominate decreases with increasing contact spacing, indicating that the channel dominates the transport mechanism at higher spacing.

To look into this non-ohmic behavior in detail, a theoretical analysis was conducted observing the measured current at two different ranges of applied voltages: low-bias ($|V_A| < 1$ V) and high-bias ($|V_A| \geq 1$ V). In the low-bias region ($|V_A| < 1$ V), the non-linearity of $I-V$ characteristics has primarily been attributed to the existence of a Schottky barrier at the contacts.[16] Fig.2 is the log(I) *vs* applied voltage (V_A) plot at three distinct temperatures and contact spacings. A linear region at $V_A < 1$ V suggests thermionic emission as the dominant conduction mechanism in the mentioned bias region. The Schottky nature of the contacts is usually verified by fitting the measured $I-V$ with Eq. (1).

$$I = I_0 \exp\left(\frac{qV}{nk_\mathrm{B}T}\right)\left[1 - \exp\left(\frac{-qV}{k_\mathrm{B}T}\right)\right] \tag{1}$$

where I is the measured current, V is the applied voltage, k_B is the Boltzmann constant, n is the ideality factor, q is the charge of electrons, and T is the temperature in Kelvin scale. I_0 is the reverse saturation current. The semi-logarithmic curve in Fig.3(a) shows that the relationship is linear, irrespective of contact spacing and temperature. Consequently, under low-bias conditions, the Schottky properties of the contact is prominent, and so thermionic emission is the major contributor in such metal-semiconductor contacts. To look into the variation of such transport mechanism with temperature, Schottky barrier height (ϕ_B) has been determined using I_0 obtained from Eq. (1)

$$I_0 = AA^*T^2 \exp\left(\frac{-q\phi_\mathrm{B}}{k_\mathrm{B}T}\right) \tag{2}$$

Here, A is the contact area and A^* is the Richardson constant. The extracted Schottky barrier height (SBH) and ideality factor are depicted in Fig.3(b). With increasing temperature, the SBH increases from 0.58 eV at 25 °C to 1.18 at 300 °C, and the ideality factor changes very slightly within this temperature range. The positive temperature coefficient of ϕ_B can be attributed to the lateral inhomogeneity of the metal/p-GaN interface SBH.[33–35] Such inhomogeneity has been mathematically described by assuming a Gaussian distribution of the barrier heights at the metal-semiconductor (M/S) interface.[33,36]:

$$\phi_\mathrm{B} = \bar{\phi}_\mathrm{B0} - \frac{q\sigma_\mathrm{s}^2}{2k_\mathrm{B}T} \tag{3}$$

where $\bar{\phi}_\mathrm{B0}$ is the mean barrier height (in eV) and σ_s is the standard deviation of the distribution. According to this model, at low temperatures, the carriers possess low thermal energy, and so, the transport is characterized by lower barrier heights (BH). Conversely, at higher temperatures, more carriers attain sufficient energy to surmount the higher barrier, thus leading to the dominance of the higher BHs in transport. Consequently, the extracted SBH exhibits an increasing characteristic with increasing temperature. The observed increasing trend of extracted BH with temperature presented in this work can be elucidated by invoking a Gaussian distribution characterized by $\bar{\phi}_\mathrm{B0}$ = 1.76 eV and $\sigma_\mathrm{s} = 0.25$ eV.

When the voltage, $|V_A| > 1$ V, the I-V characteristic deviates from Eq.(1). In this bias range, the $I-V$ becomes non-linear and non-exponential, following the form: $I \propto V^m$ as depicted in Fig.2. For a back-to-back Schottky barrier transport, the I-V is linear in the low bias and exhibits saturation at higher bias. However, the observed $I-V$ does not quantitatively align with such description, ascertaining that the non-linearity is not due to the Schottky property of the contact. Furthermore, as shown in Fig.2, for $V_A > 1$ V, $\log(I)$ is no longer proportional to V_A. Rather, $\log(I)$ follows a logarithmic rela-

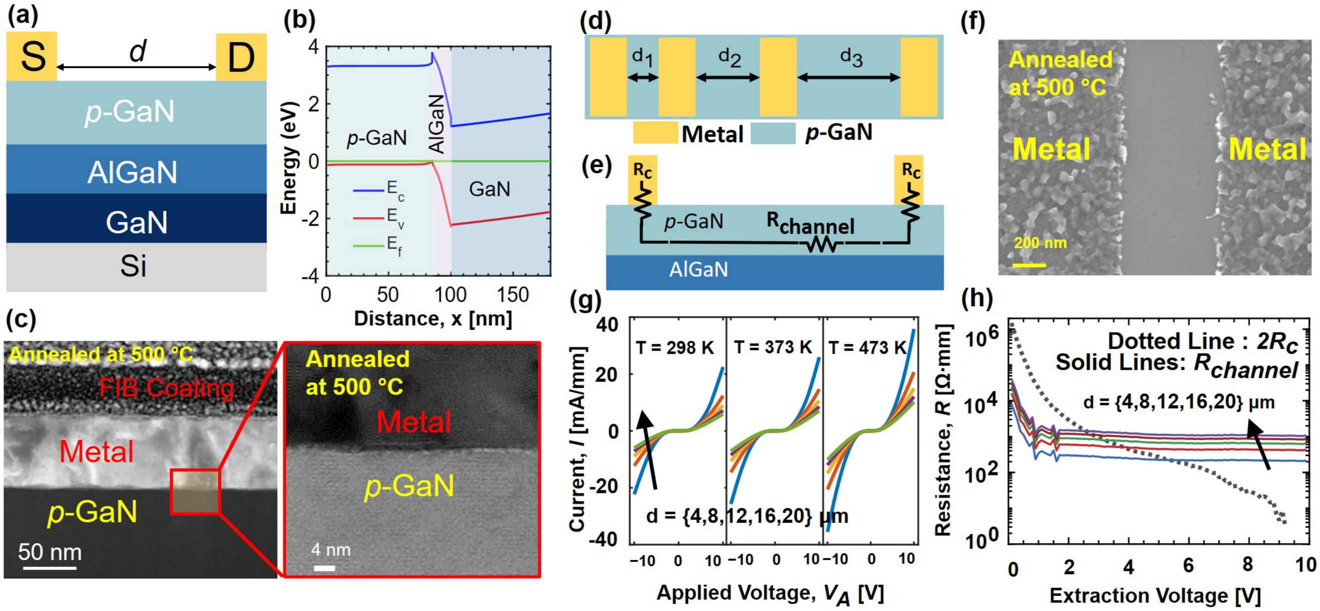

FIG. 1. (a) Schematic diagram of the p-GaN/AlGaN/GaN epitaxial structure. (b) Simulated energy band diagram of a standard p-GaN/AlGaN/GaN epitaxial structure. (c) TEM image of the cross-sectional view of the Ru-*p*-GaN contact after annealing at 500°C.(d) Schematic representation of linear TLM pads. d_1, d_2, d_3 denote the contact spacings between the linear TLM pads. (e) A schematic diagram showing two contacts to a diffused semiconductor layer, with the contact resistances (R_c) and the semiconductor/channel ($R_{channel}$) resistance indicated. (f) SEM image of the Top view of LTLM structure. (g) *I-V* characteristics of LTLM measurement at various temperatures. (h) Extracted total contact resistance ($2R_c$) and channel resistance ($R_{channel}$) for different contact spacings.

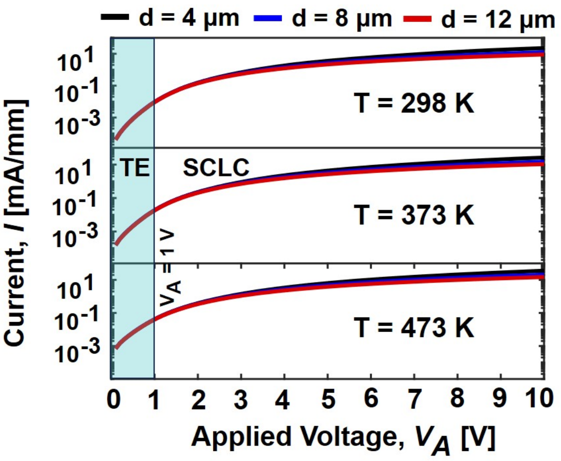

FIG. 2. Measured LTLM current *vs.* V_A plotted in semi-logarithm scale. The linear region at $V_A < 1$ V suggests thermionic emission (TE) transport region, whereas, at $V_A > 1$ V, the relation between semi-logarithmic current and applied voltage is non-linear, suggesting the current conduction mechanism is different from TE theory and follows a power law dependence on bias-voltage.

tionship with V_A, indicating a power-law dependence of current within this region. Such power law dependence of current on applied voltage is a distinctive characteristic of SCLC conduction in insulators and wide-bandgap semiconductors in the presence of shallow or deep-level trap states and thermally generated carriers.[37]

The trap-centers originating from impurities and defects will restrict the motion of a fraction of the injected carriers by capturing them and thereby influencing the transport mechanism.[38] Consequently, the trap density and distribution of the trap center significantly impact the *I-V* characteristics of a device along with the nature of the contacts. The exponent m in the SCLC transport relation has been investigated over the years. Depending on the carrier injection level, density, and distribution of trap-centers, the exponent ranges from 1.5 to a very high value. The reported ranges of exponents for various cases have been given in Table I.

Ideally, the exponent in SCLC conduction in solids is 2 according to Mott-Gurney theory;[44] however, in the presence of trap-states, the exponent (m) can exceed 2.[38,45] Notably, the exponent increases with an increase in unoccupied trap states.[38] To determine the exponent, m, the measured *I-V* data for different contact-spacings at different temperatures were fitted, attaining an R-square value exceeding 99%, which demonstrates an excellent fitting. Due to the Schottky nature of the p-GaN contacts, a significant voltage drop occurs at the contact. However, at higher bias and larger contact spacing, the channel resistance becomes order of magnitude higher than the contact resistance, thereby reducing the impact of contact voltage drop. Under these conditions, the power-law fitting yields a very high R-square value (approximately 99%), confirming the SCLC nature of the transport. Furthermore, this methodology is consistent with the previously reported approaches to extract the voltage exponent of the SCLC conduction.[40,43,46] The fitting result for $d = 4$ μm

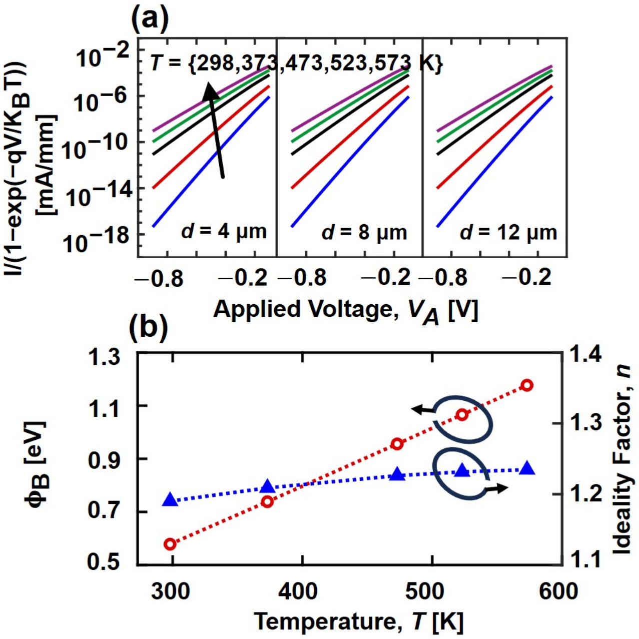

FIG. 3. (a) Examination of the low voltage region of the $I-V$ curves ($|V_A| < 1$ V) showing perfect Schottky nature at all contact spacings and temperatures. (b) Dependence of Schottky barrier height (ϕ_B) and ideality factor (n) on temperature. ϕ_B exhibits an increasing variation while n remains almost constant over the range of temperatures considered.

TABLE I. Reported Exponent (m) of $I \propto V^m$ relation in SCLC Transport.

Material/Platform	SCLC Exponent
Free Space[18]	3/2
Trap-free Solids[18]	2
Free Space and Solid[19]	[3/2, 2]
Free Space and Trap Filled Solid[20]	can be greater than 2 and in between 3/2 and 2 depending on the traps.
Ferroelectric Thin Film[39]	1.99
GaN Schottky Diodes[38]	2 - 22
GaN Nanorods[40]	2
Gate Current of GaN HEMT[41]	2
SiO_2 Nanogap Triode[42]	1.8
AlGaN/GaN UV LED[43]	2.5 - 3.46
Gate current of p-GaN Gate HEMT[21]	2.9 - 10
This Work (p-GaN/AlGaN/GaN TLM Structure)	**2 - 4**

and $d = 16$ μm at $T = 298$ K have been depicted in Fig.4 (a). Interestingly, in the voltage range of $(1 < |V_A| < 3)$ V, both 4 μm and 16 μm devices exhibit exponent exceeding 2. Beyond a certain voltage (~ 4 V), the exponents decrease and become less than 3. The higher exponent in the range, $(1 < |V_A| < 3)$ V, suggests the existence of a substantial amount of unoccupied trap states distributed in energy within the samples.[46] It has been reported that the unionized acceptor dopants can also act as hole trap centers.[47] Thus, owing to their high activation energy, the unionized Mg dopant can result in trap states.

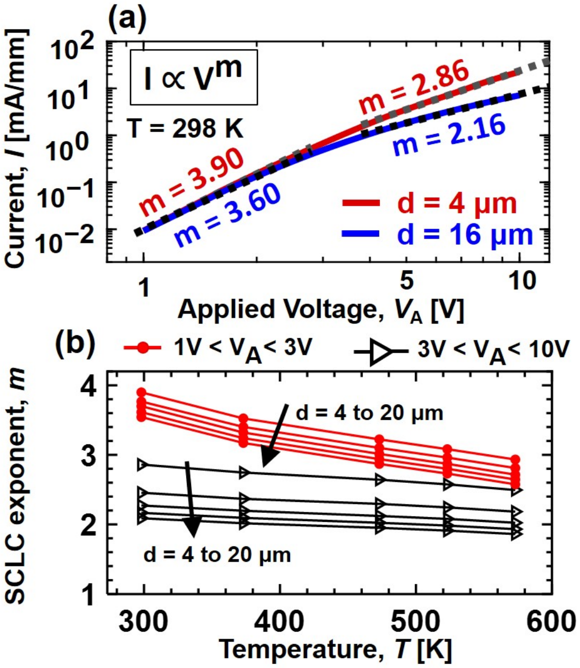

FIG. 4. (a) The power law I-V fitting for $d = 4$ μm and $d = 16$ μm at $T = 25$ °C is shown in log-log scale. The voltage exponent (m) is higher than 2 in the voltage region $(1 < V_A < 3)$ V, indicating SCLC nature. At higher voltages (higher electric field), field-induced ionization of Mg leads to the activation of acceptors in the bulk semiconductor, resulting in a reduction in m. For $d = 16$ μm, $m \sim 2$ is an indication of almost a trap-free solid. (b) The variation of SCLC exponent (m) with respect to temperature. A decreasing nature of m is observed at high temperatures due to higher activation of acceptors and higher occupation of traps.

At higher bias, i.e., $(3 < |V_A| < 10)$ V, the exponents decrease for different spacing and temperature. For instance, the exponent for $d = 4$ μm decreases from 3.95 to 2.75 within this voltage range. A similar phenomenon is evident for devices with different contact spacing as well. This decrease can be elucidated with the phenomenon field-induced acceptor ionization.[48] Increasing bias voltage results in a higher electric field, leading to an increase in the concentrations of ionized Mg-acceptors. Therefore, the exponent values decrease within this bias range. The exponents extracted from the p-GaN/AlGaN/GaN sample in this work agree well with previously reported values on SCLC conduction [Table I].

The temperature and contact-spacing dependence of the exponent is illustrated in Fig.4(b). Apparently, the exponent decreases with increased spacings. We postulate that SCLC is modulated by contact transport in short devices, with its effect diminishing in longer devices. Consequently, the exponent becomes nearly constant (the variation is within 5%) at devices with higher d. At higher temperatures, the exponent exhibits a consistent decline across all contact-spacing and voltage ranges. This is primarily attributed to the increased free carrier concentration due to the higher activation of Mg dopants with increased temperature. Consequently, the unoccupied deep-level traps have a higher probability of becoming filled and so the trap-filled SCLC tends to be less dominant. Eventually, at very high temperatures, the exponent in the bias range ($3V < V_A < 10V$) converges to 2, indicating that all the traps are occupied due to the thermal activation of the acceptors.

In summary, the current transport mechanisms in *p*-GaN/AlGaN/GaN heterostructure has been comprehensively investigated based on the analysis of the non-linear *I-V* characteristics of LTLM structure. The study's outcomes reveal the co-existence of two different current conduction mechanisms : TE and SCLC, across the observed voltage range for varied pad spacings. The exponent in the characteristic SCLC equation, $I \propto V^m$, exhibits a decreasing trend beyond a certain bias voltage, indicating the phenomenon of field-induced acceptor ionization. Furthermore, analysis at different temperature shows that SBH increases with temperature in TE emission region. In SCLC region, with increase in temperature, higher thermal activation of Mg-acceptors eventually leads to a trap-free SCLC conduction. It is anticipated that the insights gained from the analysis presented in this paper will contribute to a deeper understanding of the fundamental hole transport physics in *p*-GaN-based devices and will have implications for their performance optimization.

This work was supported in part by the Bangladesh University of Engineering and Technology; and Information and Communication Technology (ICT) Division, Government of Bangladesh. The authors thank Aric Mahbub for his valuable discussion. Q. Xie, J. Niroula, and T. Palacios acknowledge support in part by Samsung Electronics Co., Ltd. (Award No. 033517-00001); Qualcomm Inc. (Award No. MAS-492857); and Air Force Office of Scientific Research (Award No. FA9550-22-1-0367). Device fabrication was conducted at MIT.nano, Massachusetts Institute of Technology.

AUTHOR DECLARATIONS

Conflict of Interest

The authors have no conflicts to disclose.

DATA AVAILABILITY

The data that support the findings of this study are available within the article.

REFERENCES

[1] H. Amano, Y. Baines, E. Beam, M. Borga, T. Bouchet, P. R. Chalker, M. Charles, K. J. Chen, N. Chowdhury, R. Chu, *et al.*, "The 2018 GaN power electronics roadmap," Journal of Physics D: Applied Physics **51**, 163001 (2018).

[2] U. K. Mishra, L. Shen, T. E. Kazior, and Y.-F. Wu, "Gan-based rf power devices and amplifiers," Proceedings of the IEEE **96**, 287–305 (2008).

[3] Q. Xie, M. Yuan, J. Niroula, B. Sikder, J. A. Greer, N. S. Rajput, N. Chowdhury, and T. Palacios, "Highly scaled gan complementary technology on a silicon substrate," IEEE Transactions on Electron Devices **70**, 2121–2128 (2023).

[4] S. J. Bader, H. Lee, R. Chaudhuri, S. Huang, A. Hickman, A. Molnar, H. G. Xing, D. Jena, H. W. Then, N. Chowdhury, *et al.*, "Prospects for wide bandgap and ultrawide bandgap cmos devices," IEEE Transactions on Electron Devices **67**, 4010–4020 (2020).

[5] G. Tang, A. M. Kwan, R. K. Wong, J. Lei, R. Su, F. Yao, Y. Lin, J. Yu, T. Tsai, H. Tuan, *et al.*, "Digital integrated circuits on an e-mode gan power hemt platform," IEEE Electron Device Letters **38**, 1282–1285 (2017).

[6] Y. Cai, Z. Cheng, Z. Yang, C. W. Tang, K. M. Lau, and K. J. Chen, "High-temperature operation of algan/gan hemts direct-coupled fet logic (dcfl) integrated circuits," IEEE electron device letters **28**, 328–331 (2007).

[7] H. Su, T. Zhang, S. Xu, H. Tao, Y. Gao, X. Liu, L. Xie, P. Xiang, K. Cheng, Y. Hao, *et al.*, "An energy-band modulated p-gan/ingan/aln p-channel mesfet with high ion/ioff ratio and steep subthreshold swing," Applied Physics Letters **124** (2024).

[8] Y. Zhang, Z. Sun, W. Wang, Y. Liang, M. Cui, Y. Zhao, H. Wen, and W. Liu, "Low-resistance ni/ag contacts on gan-based p-channel heterojunction field-effect transistor," IEEE Transactions on Electron Devices **70**, 31–35 (2022).

[9] J. Tang, Z. Jiang, C. Wang, J. Chen, H. Chen, Y. Zhang, Z. Zheng, X. Wang, J. Ma, J. Zhao, *et al.*, "Bipolar p-fet with enhanced conduction capability on e-mode gan-on-si hemt platform," in *2023 International Electron Devices Meeting (IEDM)* (IEEE, 2023) pp. 1–4.

[10] N. Chowdhury, Q. Xie, and T. Palacios, "Tungsten-gated gan/algan p-fet with i max> 120 ma/mm on gan-on-si," IEEE Electron Device Letters **43**, 545–548 (2022).

[11] N. Chowdhury, Q. Xie, and T. Palacios, "Self-aligned e-mode gan p-channel finfet with ion> 100 ma/mm and ion/ioff> 10^7," IEEE Electron Device Letters **43**, 358–361 (2022).

[12] T. T. Mnatsakanov, M. E. Levinshtein, L. I. Pomortseva, S. N. Yurkov, G. S. Simin, and M. A. Khan, "Carrier mobility model for gan," Solid-State Electronics **47**, 111–115 (2003).

[13] W. Götz, N. Johnson, J. Walker, D. Bour, and R. Street, "Activation of acceptors in mg-doped gan grown by metalorganic chemical vapor deposition," Applied Physics Letters **68**, 667–669 (1996).

[14] Y. Park and H. Kim, "Carrier transport and effective barrier height of low resistance metal contact to highly mg-doped p-gan," Applied physics express **4**, 085701 (2011).

[15] Y. Park, K.-S. Ahn, and H. Kim, "Carrier transport mechanism of ni/ag/pt contacts to p-type gan," IEEE transactions on electron devices **59**, 680–684 (2012).

[16] C. Tang, C. Fu, Y. Jiang, M. He, C. Deng, K. Wen, J. He, P. Wang, F. Du, Y. Zhang, *et al.*, "Carrier transport mechanism of mg/pt/au ohmic contact on p-gan/algan/gan platform with ultra-low resistivity," Applied Physics Letters **123** (2023).

[17] P. Murgatroyd, "Theory of space-charge-limited current enhanced by frenkel effect," Journal of Physics D: Applied Physics **3**, 151 (1970).

[18] P. Zhang, Á. Valfells, L. Ang, J. Luginsland, and Y. Lau, "100 years of the physics of diodes," Applied Physics Reviews **4** (2017).

[19] W. Chandra and L. Ang, "Space charge limited current in a gap combined of free space and solid," Applied Physics Letters **96** (2010).

[20] Y. B. Zhu, K. Geng, Z. S. Cheng, and R. H. Yao, "Space-charge-limited current injection into free space and trap-filled solid," IEEE transactions on plasma science **49**, 2107–2112 (2021).

[21] Y. Shi, Q. Zhou, Q. Cheng, P. Wei, L. Zhu, D. Wei, A. Zhang, W. Chen, and B. Zhang, "Bidirectional threshold voltage shift and gate leakage in 650 v p-gan algan/gan hemts: The role of electron-trapping and hole-injection," in *2018 IEEE 30th International Symposium on Power Semiconductor Devices and ICs (ISPSD)* (IEEE, 2018) pp. 96–99.

[22] J. A. del Alamo and E. S. Lee, "Stability and reliability of lateral gan power field-effect transistors," IEEE Transactions on Electron Devices **66**, 4578–4590 (2019).

[23] E. S. Lee, J. Joh, D. S. Lee, and J. A. del Alamo, "Impact of gate offset on pbti of p-gan gate hemts," in *2022 IEEE International Reliability Physics Symposium (IRPS)* (IEEE, 2022) pp. P21–1.

[24] Q. Xie, J. Niroula, N. S. Rajput, M. Yuan, S. Luo, K. Fu, M. F. Isamotu, R. H. Palash, B. Sikder, S. R. Eisner, *et al.*, "Device and material investigations of gan enhancement-mode transistors for venus and harsh environments," Applied Physics Letters **124** (2024).

[25] H.-B. Do, J. Zhou, and M. M. De Souza, "Origins of the schottky barrier to a 2dhg in a au/ni/gan/algan/gan heterostructure," ACS Applied Electronic Materials **4**, 4808–4813 (2022).

[26] Y. H. Ng, Z. Zheng, L. Zhang, R. Liu, T. Chen, S. Feng, Q. Shao, and K. J. Chen, "Distribution and transport of holes in the p-gan/algan/gan heterostructure," Applied Physics Letters **123** (2023).

[27] Z. Zheng, W. Song, L. Zhang, S. Yang, H. Xu, R. K.-Y. Wong, J. Wei, and K. J. Chen, "Enhancement-mode gan p-channel mosfets for power integration," in *2020 32nd International Symposium on Power Semiconductor Devices and ICs (ISPSD)* (2020) pp. 525–528.

[28] N. Chowdhury, J. Lemettinen, Q. Xie, Y. Zhang, N. S. Rajput, P. Xiang, K. Cheng, S. Suihkonen, H. W. Then, and T. Palacios, "P-channel gan transistor based on p-gan/algan/gan on si," IEEE Electron Device Letters **40**, 1036–1039 (2019).

[29] Q. Xie, *p-GaN Platform for Next-Generation GaNComplementary Transistors and Circuits*, Ph.D. thesis, Massachusetts Institute of Technology (2024).

[30] T. Arunagiri, Y. Zhang, O. Chyan, M. El-Bouanani, M. Kim, K. Chen, C. Wu, and L. Chen, "5nm ruthenium thin film as a directly plateable copper diffusion barrier," Applied Physics Letters **86** (2005).

[31] M. Pawlak, M. Popovici, J. Swerts, K. Tomida, M.-S. Kim, B. Kaczer, K. Opsomer, M. Schaekers, P. Favia, H. Bender, *et al.*, "Enabling 3x nm dram: Record low leakage 0.4 nm eot mim capacitors with novel stack engineering," in *2010 International Electron Devices Meeting* (IEEE, 2010) pp. 11–7.

[32] S. Wahid, N. Chowdhury, M. K. Alam, and T. Palacios, "Barrier heights and fermi level pinning in metal contacts on p-type gan," Applied Physics Letters **116** (2020).

[33] N. Yıldırım, K. Ejderha, and A. Turut, "On temperature-dependent experimental iv and cv data of ni/n-gan schottky contacts," Journal of Applied Physics **108** (2010).

[34] N. Subramaniyam, M. Sopanen, H. Lipsanen, C.-H. Hong, and E.-K. Suh, "Inhomogeneous barrier height analysis of (ni/au)–inalgan/gan schottky barrier diode," Japanese Journal of Applied Physics **50**, 030201 (2011).

[35] T. Maeda, M. Okada, M. Ueno, Y. Yamamoto, T. Kimoto, M. Horita, and J. Suda, "Temperature dependence of barrier height in ni/n-gan schottky barrier diode," Applied Physics Express **10**, 051002 (2017).

[36] J. H. Werner and H. H. Güttler, "Barrier inhomogeneities at schottky contacts," Journal of applied physics **69**, 1522–1533 (1991).

[37] P. Zhang, Y. S. Ang, A. L. Garner, Á. Valfells, J. Luginsland, and L. Ang, "Space–charge limited current in nanodiodes: Ballistic, collisional, and dynamical effects," Journal of Applied Physics **129** (2021).

[38] X. Shen, D. Zhao, Z. Liu, Z. Hu, H. Yang, and J. Liang, "Space-charge-limited currents in gan schottky diodes," Solid-state electronics **49**, 847–852 (2005).

[39] J. Sun, X. Zheng, W. Yin, M. Tang, and W. Li, "Space-charge-limited leakage current in high dielectric constant and ferroelectric thin films considering the field-dependent permittivity," Applied Physics Letters **97** (2010).

[40] A. A. Talin, F. Léonard, B. Swartzentruber, X. Wang, and S. D. Hersee, "Unusually strong space-charge-limited current in thin wires," Physical review letters **101**, 076802 (2008).

[41] W. Xu, H. Rao, and G. Bosman, "Evidence of space charge limited flow in the gate current of algan/gan high electron mobility transistors," Applied Physics Letters **100** (2012).

[42] S. Srisonphan, "Field effect-controlled space-charge limited emission triode with nanogap channels," IEEE Electron Device Letters **42**, 1540–1543 (2021).

[43] J. H. Park, J. K. Kim, and J. Cho, "Observation of space-charge-limited current in algan/gan ultraviolet light-emitting diodes," Materials Letters **214**, 217–219 (2018).

[44] N. F. Mott and R. W. Gurney, "Electronic processes in ionic crystals," (No Title) (1948).

[45] P. Mark and W. Helfrich, "Space-charge-limited currents in organic crystals," Journal of Applied Physics **33**, 205–215 (1962).

[46] B. Simpkins, M. Mastro, C. Eddy, J. Hite, and P. Pehrsson, "Space-charge-limited currents and trap characterization in coaxial algan/gan nanowires," Journal of Applied Physics **110** (2011).

[47] M. Lu, H. T. Nicolai, G.-J. A. Wetzelaer, and P. W. Blom, "Effect of n-type doping on the hole transport in poly (p-phenylene vinylene)," Journal of Polymer Science Part B: Polymer Physics **49**, 1745–1749 (2011).

[48] N. Chowdhury, Q. Xie, J. Niroula, N. S. Rajput, K. Cheng, H. W. Then, and T. Palacios, "Field-induced acceptor ionization in enhancement-mode gan p-mosfets," in *2020 IEEE International Electron Devices Meeting (IEDM)* (IEEE, 2020) pp. 5–5.

View publication stats